

J/Ψ suppression in an expanding equilibrium hadron gas *

Dariusz Prorok and Ludwik Turko
*Institute of Theoretical Physics, University of Wrocław,
Pl. Maksa Borna 9, 50-204 Wrocław, Poland*
(February 17, 2000)

We consider an ideal gas of massive hadrons in thermal and chemical equilibrium. The finite-size gas expands longitudinally in accordance with Bjorken law. Also the transverse expansion in a form of the rarefaction wave is considered. We show that J/Ψ suppression in such an environment, when combined with the disintegration in nuclear matter, agrees qualitatively well with NA38 and NA50 data.

I. INTRODUCTION

Since the paper of Matsui and Satz [1] there is a steady interest in the problem of J/Ψ suppression in a heavy-ion collision. The question is if this suppression can be treated as a signature for a quark-gluon plasma or if it can be explained by J/Ψ absorption in a hadron gas which appears in the central rapidity region (CRR) of the collision [2–5].

In the following paper we shall continue our previous investigations [6] into the problem of J/Ψ suppression observed in a heavy-ion collision (for experimental data see e.g. [7] and references therein). Now, we shall focus on the dependence of the suppression on the initial energy density reached in the CRR.

In our model, J/Ψ suppression is the result of a $c\bar{c}$ state absorption in a dense hadronic matter through interactions of the type

$$c\bar{c} + h \longrightarrow D + \bar{D} + X, \quad (1)$$

where h denotes a hadron, D is a charm meson and X means a particle which is necessary to conserve the charge, baryon number or strangeness. The hadronic matter is in a state of an ideal gas of massive hadrons in thermal and chemical equilibrium and consists of all species up to Ω^- baryon. Time evolution is given here by conservation laws combined with assumptions about the space-time structure of the system. A corresponding equation of state of the ideal gas makes then possible to express gas parameters such as temperature and chemical potentials as functions of time.

An ideal gas of real hadrons has a very interesting feature: it cools much slower than a pion gas when expands longitudinally. We have checked numerically that for the initial energy densities ϵ_0 corresponding to initial temperatures T_0 of the order of 200 MeV and for the freeze-out $T_{f.o.}$ not lower than about 100 MeV, the time dependence of the temperature of the expanding gas still keeps the well-known form $T(t) = T_0 \cdot t^{-a}$ (we put $t_0 = 1fm$). Only the exponent a changes from $\frac{1}{3}$ for massless pions to the values $\frac{1}{5.6} - \frac{1}{5.3}$ for massive realistic hadrons. As a result, the time of the freeze-out $t_{f.o.}$ is much greater for the hadron gas than for the pion one. For instance, when we take $T_0 = 200MeV$ and $T_{f.o.} = 140MeV$ we obtain $t_{f.o.} = 7.37fm$ ($a = \frac{1}{5.6}$) for the hadron gas and $t_{f.o.} = 2.9fm$ ($a = \frac{1}{3}$) for the pion gas. The lower $T_{f.o.}$, the stronger difference. For $T_0 = 200MeV$ and $T_{f.o.} = 100MeV$ we have $t_{f.o.} = 48.5fm$ ($a = \frac{1}{5.6}$) for the hadron gas and $t_{f.o.} = 8fm$ ($a = \frac{1}{3}$) for the pion gas. This has a direct consequence for J/Ψ suppression: the longer the system lasts, the deeper suppression causes (see Fig. 1).

*Work partially supported by the Polish Committee for Scientific Research under contract KBN - 2 P03B 030 18

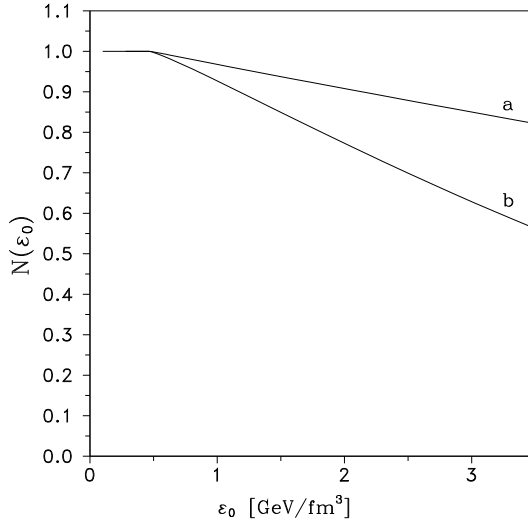


FIG. 1. comparison of suppression of the pure J/Ψ 's in the cooling hadron gas for two values of the power a in approximation $T(t) \cong T_0 \cdot t^{-a}$: a) $a = \frac{1}{3}$; b) $a = \frac{1}{5.6}$

We are going to calculate a survival factor for J/Ψ when new, more realistic conditions are taken into account. We consider a hadronic gas which is produced in the CRR region. This gas expands both longitudinally and transversely. The longitudinal expansion is a traditional adiabatic hydrodynamical evolution [8], the transverse expansion is considered as the rarefaction wave. An initial energy density depends now on the impact parameter b and on the geometry of the collision.

II. THE EXPANDING HADRON GAS

For an ideal hadron gas in thermal and chemical equilibrium, which consists of l species of particles, energy density ϵ , baryon number density n_B , strangeness density n_S and entropy density s read ($\hbar = c = 1$ always)

$$\epsilon = \frac{1}{2\pi^2} \sum_{i=1}^l (2s_i + 1) \int_0^\infty \frac{dpp^2 E_i}{\exp\left\{\frac{E_i - \mu_i}{T}\right\} + g_i}, \quad (2a)$$

$$n_B = \frac{1}{2\pi^2} \sum_{i=1}^l (2s_i + 1) \int_0^\infty \frac{dpp^2 B_i}{\exp\left\{\frac{E_i - \mu_i}{T}\right\} + g_i}, \quad (2b)$$

$$n_S = \frac{1}{2\pi^2} \sum_{i=1}^l (2s_i + 1) \int_0^\infty \frac{dpp^2 S_i}{\exp\left\{\frac{E_i - \mu_i}{T}\right\} + g_i}, \quad (2c)$$

$$s = \frac{1}{6\pi^2 T^2} \sum_{i=1}^l (2s_i + 1) \int_0^\infty \frac{dpp^4 (E_i - \mu_i) \exp\left\{\frac{E_i - \mu_i}{T}\right\}}{E_i \left(\exp\left\{\frac{E_i - \mu_i}{T}\right\} + g_i\right)^2}, \quad (2d)$$

where $E_i = (m_i^2 + p^2)^{1/2}$ and m_i , B_i , S_i , μ_i , s_i and g_i are the mass, baryon number, strangeness, chemical potential, spin and a statistical factor of specie i respectively (we treat an antiparticle as a different specie). And $\mu_i = B_i \mu_B + S_i \mu_S$, where μ_B and μ_S are overall baryon number and strangeness chemical potentials respectively.

We shall work here within the usual timetable of the events in the CRR of a given ion collision (for more details see e.g. [5]). We fix $t = 0$ at the moment of the maximal overlap of the nuclei. After half of the time the nuclei need to cross each other, matter appears in the CRR. We assume that soon thereafter matter thermalizes and this

moment, t_0 , is estimated at about 1 fm [5,8]. Then matter starts to expand and cool and after reaching the freeze-out temperature it is no longer a thermodynamical system. We denote this moment as $t_{f.o.}$. As we have already mentioned in the introduction, this matter is the hadron gas, which consists of all hadrons up to Ω^- baryon. The expansion proceeds according to the relativistic hydrodynamics equations and for the longitudinal component we have the following solution (for details see e.g. [8,9])

$$s(t) = \frac{s_0 t_0}{t}, \quad n_B(t) = \frac{n_B^0 t_0}{t}, \quad (3)$$

where s_0 and n_B^0 are initial densities of the entropy and the baryon number respectively. The superimposed transverse expansion has the form of the rarefaction wave moving radially inward with a sound velocity c_s [8,10].

To obtain the time dependence of temperature and baryon number and strangeness chemical potentials one has to solve numerically equations (2b - 2d) with s , n_B and n_S given as time dependent quantities. For $s(t)$, $n_B(t)$ we have expressions (3) and $n_S = 0$ since we put the overall strangeness equal to zero during all the evolution (for more details see [11]).

The sound velocity squared is given by $c_s^2 = \frac{\partial P}{\partial \epsilon}$ and can be evaluated numerically [11,12].

III. J/Ψ ABSORPTION IN HADRONIC MATTER

In a high energy heavy-ion collision, charmonium states are produced mainly through gluon fusion and it takes place during the overlap of colliding nuclei. For the purpose of our model, we shall assume that all $c\bar{c}$ pairs are created at the moment $t = 0$. Before the fusion, gluons can suffer multiple elastic scattering on nucleons and gain some additional transverse momentum in this way [13–15]. This manifests for instance in the observed broadening of the p_T distribution of J/Ψ [16]. Following [17], we express this effect by the transverse momentum distribution of the charmonium states of the form

$$g(p_T, \epsilon_0) = \frac{2p_T}{\langle p_T^2 \rangle_{J/\Psi}^{AB}(\epsilon_0)} \cdot \exp \left\{ -\frac{p_T^2}{\langle p_T^2 \rangle_{J/\Psi}^{AB}(\epsilon_0)} \right\}, \quad (4)$$

where $\langle p_T^2 \rangle_{J/\Psi}^{AB}(\epsilon_0)$ is the mean squared transverse momentum of J/Ψ gained in an A-B collision with the initial energy density ϵ_0 . The momentum can be expressed as (for details see [18])

$$\langle p_T^2 \rangle_{J/\Psi}^{AB}(\epsilon) = \langle p_T^2 \rangle_{J/\Psi}^{pp} + K \cdot \epsilon, \quad (5)$$

with $K = 0.27 \text{ fm}^3 \cdot \text{GeV}$ and $\langle p_T^2 \rangle_{J/\Psi}^{pp} = 1.24 \text{ GeV}^2$ taken from a fit to the J/Ψ data of NA38 Collaboration [18]. The expression in (4) is normalized to unity and is treated as the initial momentum distribution of charmonium states here.

For the simplicity of our model, we shall assume that all charmonium states are completely formed and can be absorbed by the constituents of a surrounding medium from the moment of creation. It means that we neglect a whole complex process of J/Ψ formation as presented in [19,20]. The main feature of the above-mentioned process is that, soon after the moment of production, the $c\bar{c}$ pair binds a soft gluon and creates a pre-resonance $c\bar{c} - g$ state, from which, after a time of the order of 0.3 fm, a physical charmonium state is formed. This means that the possible nuclear absorption of charmonium is, in fact, the absorption of the $c\bar{c} - g$ state. But the latest has the cross-section $\sigma_{abs} = 7.3 \text{ mb}$, which is much higher than $J/\Psi - \text{Nucleon}$ absorption cross-section $\sigma_{\psi N} \cong 3 - 5 \text{ mb}$ obtained from p-A data [16,21,22]. This justifies our assumption: taking into account $c\bar{c} - g$ absorption instead of charmonium disintegration in the nuclear matter would only strengthen J/Ψ suppression.

According to the above assumption, charmonium states can be absorbed first in the nuclear matter and soon later, when the matter appears in the CRR, in the hadron gas. Since these two processes are separated in time, J/Ψ survival factor for a heavy-ion collision with the initial energy density ϵ_0 , may be written in the form

$$\mathcal{N}(\epsilon_0) = \mathcal{N}_{n.m.}(\epsilon_0) \cdot \mathcal{N}_{h.g.}(\epsilon_0), \quad (6)$$

where $\mathcal{N}_{n.m.}(\epsilon_0)$ and $\mathcal{N}_{h.g.}(\epsilon_0)$ are J/Ψ survival factors in the nuclear matter and the hadron gas, respectively. For $\mathcal{N}_{n.m.}(\epsilon_0)$ we have the usual approximation [22–24]

$$n.m.(\epsilon_0) \cong \exp \{ -\sigma_{\psi N} \rho_0 L \}, \quad (7)$$

where ρ_0 is the nuclear matter density and L the mean path length of the J/Ψ through the colliding nuclei. For the last quantity, we use the expression given in [24]:

$$L(b) = \frac{1}{2\rho_0 T_{AB}} \int d^2\vec{s} T_A(\vec{s}) T_B(\vec{s} - \vec{b}) \left[T_A(\vec{s}) + T_B(\vec{s} - \vec{b}) \right], \quad (8)$$

where $T_{AB}(b) = \int d^2\vec{s} T_A(\vec{s}) T_B(\vec{s} - \vec{b})$, $T_A(\vec{s}) = \int dz \rho_A(\vec{s}, z)$ is the nuclear density profile function, $\rho_A(\vec{s}, z)$ the nuclear matter density distribution and b the impact parameter. How to obtain ϵ_0 as a function of b will be presented further.

To estimate $\mathcal{N}_{h.g.}(\epsilon_0)$ we follow the description presented in [6]. We shall focus on the plane $z = 0$ (z is a collision axis) and put J/Ψ longitudinal momentum equal to zero. Now the p_T -dependent J/Ψ survival factor $\mathcal{N}_{h.g.}(p_T)$ is given by (for details see [6])

$$\mathcal{N}_{h.g.}(p_T) = \int d^2\vec{s} f_0(s, p_T) \exp \left\{ - \int_{t_0}^{t_f} dt \sum_{i=1}^l \int \frac{d^3\vec{q}}{(2\pi)^3} f_i(\vec{q}, t) \sigma_i v_{rel,i} \frac{p_\nu q'_i}{E E'_i} \right\}, \quad (9)$$

where the sum in the power is over all taken species of scatters (hadrons), $p^\nu = (E, \vec{p}_T)$ and $q'_i = (E'_i, \vec{q})$ are four momenta of J/Ψ and hadron specie i respectively, $\vec{v} = \vec{p}_T/E$ is the velocity of the former, σ_i states for the absorption cross-section of $J/\Psi - h_i$ scattering and $v_{rel,i}$ is the relative velocity of h_i hadron with respect to J/Ψ . When M denotes J/Ψ mass, $M = 3097$ MeV, $v_{rel,i}$ reads

$$v_{rel,i} = \left(1 - \frac{m_i^2 M^2}{(p_\nu q'_i)^2} \right)^{\frac{1}{2}}. \quad (10)$$

The upper limit of the time integral in (9), t_f , is equal to $t_{f.o.}$ or to t_{esc} – the moment of leaving by a given J/Ψ of the hadron medium, if the final-size effects are considered and $t_{esc} < t_{f.o.}$. For σ_i we have assumed that it equals zero for $(p^\nu + q'_i)^2 < (2m_D + m_X)^2$ and is constant elsewhere (m_D is a charm meson mass, $m_D = 1867$ MeV). For hadron specie i we have usual Bose-Einstein or Fermi-Dirac distribution (we neglect any possible spatial dependence here)

$$f_i(\vec{q}, t) = f_i(q, t) = \frac{2s_i + 1}{\exp \left\{ \frac{E'_i - \mu_i(t)}{T(t)} \right\} + g_i}. \quad (11)$$

In the following, we shall consider only J/Ψ initial distribution $f_0(s, p_T)$ that factorizes into $f_0(s)g(p_T)$ and the momentum distribution $g(p_T)$ will be given by (4). We assume at the first step that the transverse size of the hadron medium is much greater than $t_{f.o.}$ and also much greater than the size of the area where $f_0(s)$ is non-zero. Additionally we assume that $f_0(s)$ is uniform and normalized to unity. Note that the first assumption overestimates the suppression but the second, in the presence of the first, has no any calculable effect here. As a result, $\mathcal{N}_{h.g.}(p_T)$ simplifies to

$$\mathcal{N}_{h.g.}(p_T) = g(p_T, \epsilon_0) \cdot \exp \left\{ - \int_{t_0}^{t_{f.o.}} dt \sum_{i=1}^l \int \frac{d^3\vec{q}}{(2\pi)^3} f_i(\vec{q}, t) \sigma_i v_{rel,i} \frac{p_\nu q'_i}{E E'_i} \right\}, \quad (12)$$

To obtain $\mathcal{N}_{h.g.}(\epsilon_0)$ one needs only to integrate (12) over p_T :

$$\mathcal{N}_{h.g.}(\epsilon_0) = \int dp_T g(p_T, \epsilon_0) \cdot \exp \left\{ - \int_{t_0}^{t_{f.o.}} dt \sum_{i=1}^l \int \frac{d^3\vec{q}}{(2\pi)^3} f_i(\vec{q}, t) \sigma_i v_{rel,i} \frac{p_\nu q'_i}{E E'_i} \right\}. \quad (13)$$

Now we would like to take the final-size effects and the transverse expansion into account in our model. To do this directly, we would have to come back to the formula given by (9) and integrate it, instead of (12), over p_T . But this would involve a five-dimensional integral (the three-dimensional integral over \vec{q} simplifies to the one-dimensional one, in fact) instead of the three-dimensional integral of (13). Therefore, we need to simplify in some way the direct method just mentioned above. We shall define an average time of leaving the hadron medium by J/Ψ 's with the velocity v produced in an A-B collision at impact parameter b , $\langle t_{esc} \rangle(b, v)$. Then, we will put this quantity, instead of $t_{f.o.}$, as the upper limit of the integral over t in (13).

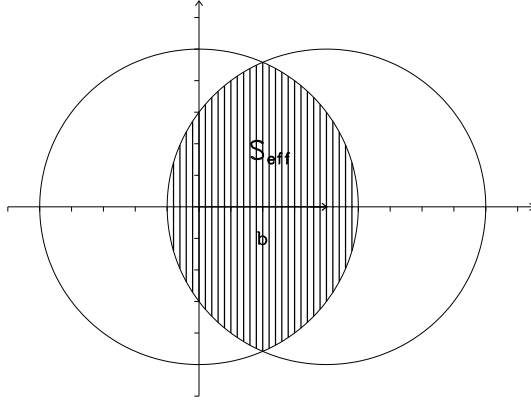


FIG. 2. View of a Pb-Pb collision at impact parameter b in the transverse plane ($z = 0$). The region where the nuclei overlap has been hatched and its area equals S_{eff} .

Let us consider an A-B collision at impact parameter b . Since we will compare final results with the latest data of NA50 which are for Pb-Pb collisions [7], we focus on the case of A=B here. So, for the collision at impact parameter b we have the situation in the plane $z = 0$ as presented in Fig. 2, where S_{eff} means the area of the overlap of the colliding nuclei. We shall assume here, that the hadron medium, which appears in the space between the nuclei after they crossed each other also has the shape of S_{eff} at t_0 in the plane $z = 0$. And additionally, the transverse expansion will start in the form of the rarefaction wave moving inward S_{eff} at t_0 . Then, for a J/Ψ which is at $\vec{r} \in S_{eff}$ at the moment t_0 and has the velocity \vec{v} we denote by t_{esc} the moment of crossing the border of the hadron gas. It means that t_{esc} is a solution of the equation $|\vec{d} + \vec{v}(t - t_0)| = R_A - c_s(t - t_0)$, where $R_A = r_0 \cdot A^{1/3}$ ($r_0 = 1.2 fm$) is the nucleus radius and $\vec{d} = \vec{r} - \vec{b}$ for the angle between \vec{r} and \vec{v} such that the J/Ψ will cross this part of the edge of the area of the hadron gas which was created by the projectile and $\vec{d} = \vec{r}$ in the opposite. Having obtain t_{esc} , we average it over the angle between \vec{r} and \vec{v} , i.e. we integrate t_{esc} over this angle and divide by 2π . Then we average the result over S_{eff} with the weight given by

$$p_{J/\Psi}(\vec{r}) = \frac{T_A(\vec{r})T_B(\vec{r} - \vec{b})}{T_{AB}(b)} \quad (14)$$

and we obtain $\langle t_{esc} \rangle(b, v)$. So, the final expression for $\mathcal{N}_{h.g.}(\epsilon_0)$ when the transverse expansion is taken into account reads

$$\mathcal{N}_{h.g.}(\epsilon_0) = \int dp_T g(p_T, \epsilon_0) \cdot \exp \left\{ - \int_{t_0}^{\langle t_{esc} \rangle} dt \sum_{i=1}^l \int \frac{d^3 \vec{q}}{(2\pi)^3} f_i(\vec{q}, t) \sigma_i v_{rel, i} \frac{p_\nu q_i^\nu}{E E_i'} \right\} . \quad (15)$$

IV. THE ENERGY DENSITY IN THE CRR

To compare our theoretical estimations for J/Ψ survival factor with the experimental data [7] we need to modify the latest so as they become ϵ_0 -dependent instead of E_T -dependent (E_T is the neutral transverse energy). To do this we will use the well-known Bjorken formula

$$\epsilon_0 = \frac{3 \cdot E_T}{\Delta \eta S_{eff} t_0} , \quad (16)$$

where $\Delta \eta$ is the pseudo-rapidity range. Using values of impact parameter b given in [7] we can calculate S_{eff} for each measured E_T bin.

In further considerations we will need the formula for the number of participating nucleons as a function of impact parameter b :

$$N_{part}(b) = \int_{S_{eff}} d^2 \vec{s} \left\{ T_A(\vec{s}) + T_B(\vec{s} - \vec{b}) \right\} . \quad (17)$$

We found out that the ratio E_T/N_{part} is almost constant and for NA50 data [7] varies from 0.28 GeV to 0.31 GeV with the average value equal roughly to 0.3 GeV and the standard deviation equal to 0.0094 GeV. Therefore we assume that for Pb-Pb collisions of NA50 the following approximation is valid:

$$E_T \cong 0.3 \cdot N_{part} . \quad (18)$$

Having put (18) into (16) we obtain ϵ_0 as a function of b

$$\epsilon_0(b) = 0.75 \cdot \frac{N_{part}(b)}{S_{eff}(b)} , \quad (19)$$

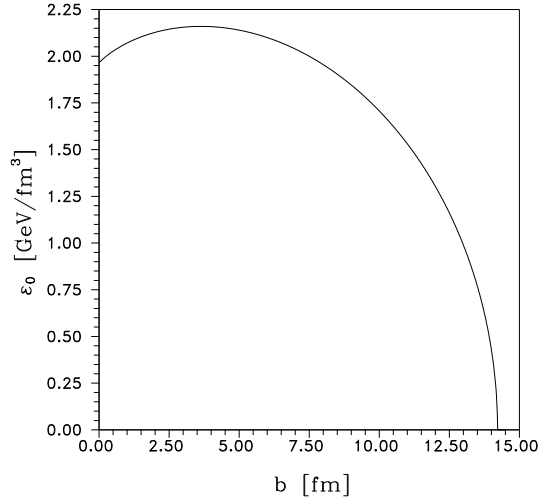


FIG. 3. The initial energy density ϵ_0 in the CRR for Pb-Pb collisions as the function of impact parameter b and for the NA50 data of 1996 run [7]

where we have also used the value $\Delta\eta = 1.2$ of NA50 [7]. The above function is depicted in Fig. 3. The behaviour in low b is the most interesting feature of $\epsilon_0(b)$. We can see that for $b \leq 7.9$ there are two different values b_1 and b_2 such that $\epsilon_0(b_1) = \epsilon_0(b_2)$. Of course, this is the result of direct application of (18) which is some approximation in fact. But nevertheless this can suggest that there is a wide range of impact parameter b for which the resulting ϵ_0 is almost constant. Using the dependence between E_T and b obtained by NA50 [7], we can state the similar for E_T , i.e. for $E_T \geq 40 - 50 \text{ GeV}$ ϵ_0 changes weakly with E_T . Also the same is true for J/Ψ suppression what could suggest that the quantity of ϵ_0 reached is the main reason for the suppression.

V. RESULTS

To evaluate formulae (13) and (15) we have to know $T(t)$, $\mu_B(t)$ and $\mu_S(t)$ and how to obtain these functions was explained in Sect. II. But to follow all that procedure we need initial values s_0 and n_B^0 . To estimate initial baryon number density n_B^0 we can use experimental results for S-S [25] or Au-Au [26,27] collisions. In the first approximation we can assume that the baryon multiplicity per unit rapidity in the CRR is proportional to the number of participating nucleons. For a sulphur-sulphur collision we have $dN_B/dy \cong 6$ [25] and 64 participating nucleons. For the central collision of lead nuclei we can estimate the number of participating nucleons at $2A = 416$, so we have $dN_B/dy \cong 39$. Having taken the initial volume in the CRR equal to $\pi R_A^2 \cdot 1 \text{ fm}$, we arrive at $n_B^0 \cong 0.25 \text{ fm}^{-3}$. This is some underestimation because the S-S collisions were at a beam energy of 200 GeV/nucleon, but Pb-Pb at 158 GeV/nucleon. From the Au-Au data extrapolation one can estimate $n_B^0 \cong 0.65 \text{ fm}^{-3}$ [26]. These values are for central collisions, and for the higher impact parameter (a more peripheral collision) the initial baryon number density should be much lower. In fact, if we apply the above-mentioned assumption, the initial baryon number density for a given collision at the impact parameter b will be proportional to the number of participating nucleons divided by S_{eff} . Therefore, $n_B^0(b)$ will have exactly the same shape as $\epsilon_0(b)$ presented in Fig. 3. As a result, only for the most peripheral collisions n_B^0 will be substantially below the value for the central one. So, to simplify numerical calculations we will keep n_B^0 constant over the all range of b and additionally, to check the possible dependence on n_B^0 , we will do

our estimations for n_B^0 substantially lower, i.e. $n_B^0 = 0.05 fm^{-3}$. According to our approximation of $n_B^0(b)$, it would correspond to the most peripheral Pb-Pb collisions, $b \geq 14 fm$.

Now, to find s_0 , first we have to solve (2a - 2c) with respect to T , μ_S and μ_B , where we put $\epsilon = \epsilon_0$, $n_B = n_B^0$ and $n_S = 0$. Then, having put T , μ_S and μ_B into (2d) we obtain s_0 . Finally, expressing left sides of (2b,2d) by (3) and after then solving (2b - 2d) numerically we can obtain T , μ_S and μ_B as functions of time. In fact, evaluating formulae (13) and (15) we do the following: first, we calculate $T = T(t)$ which turns out to be very well approximated by the expression

$$T(t) \cong T_0 \cdot t^{-a} \quad (20)$$

and then we put this approximation into (13) and (15). And for $\mu_S(t)$ and $\mu_B(t)$ in $f_i(\vec{q}, t)$ we put solutions of (2b,2c) where n_B given by (3) and $n_S = 0$ and T is given by (20). But the exponent a in (20) has proven not to be unique for the whole range of T_0 considered here. One gets different values of the initial energy density ϵ_0 for different values of the impact parameter b and for different geometry of the collision process. So b dependent a gives also b dependent freeze-out time $t_{f.o.}$. The formula (19) is calculated for different values of b and Eqs. (2a - 2c) are solved. We have evaluated the suppression factor up to $\epsilon_0 = 3.5 GeV/fm^3$. This gives e.g. the maximal possible T_0 , $T_{0,max}$, equal to $219.3 MeV$ (for $n_B^0 = 0.65 fm^{-3}$), $224 MeV$ (for $n_B^0 = 0.25 fm^{-3}$) or $224.8 MeV$ (for $n_B^0 = 0.05 fm^{-3}$).

This procedure allows to evaluate J/Ψ survival factor given by (13). Because of the lack of data, we shall assume only two types of the cross-section, the first, σ_b , for J/Ψ -baryon scattering and the second, σ_m , for J/Ψ -meson scattering. For σ_b we put $\sigma_b = \sigma_{J/\psi N}$. As far as σ_m is concerned, we assume that this cross-section is 2/3 of the corresponding cross section for baryons, which is due to the quark counting. In the following, we will use values of J/Ψ - Nucleon absorption cross-section $\sigma_{J/\psi N} \cong 3 - 5 mb$ obtained from p-A data [16,21,22]. At the beginning, to illustrate how the value of power a influences J/Ψ suppression we present in Fig. 1 two results: the first for $a = \frac{1}{3}$ (which is the exact value for a free massless gas) and the second for $a = \frac{1}{5.6}$ (which is the approximate value for the hadron gas and $T_0 \cong 200 MeV$). We can see that the suppression improves more than twice for the highest ϵ_0 indeed.

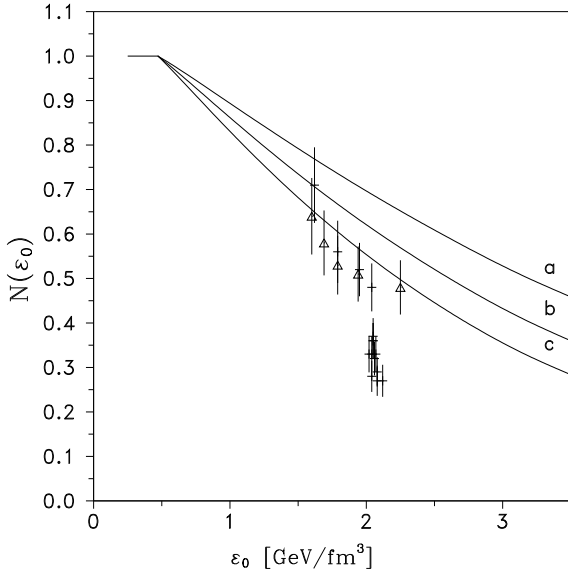


FIG. 4. J/Ψ suppression in the longitudinally expanding hadron gas with the "infinite" transverse size and for $n_B^0 = 0.25 fm^{-3}$ and $T_{f.o.} = 140 MeV$: a) $\sigma_b = 3 mb$, $\sigma_m = 2 mb$; b) $\sigma_b = 4 mb$, $\sigma_m = 2.66 mb$; c) $\sigma_b = 5 mb$, $\sigma_m = 3.33 mb$. Triangles and crosses represent the S-U data of NA38 and the Pb-Pb data of NA50 Collaborations [7], respectively.

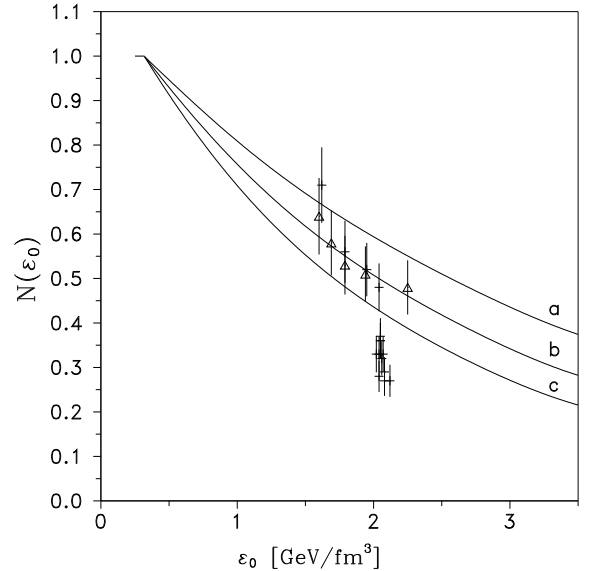


FIG. 5. Same as Fig. 4 but for $T_{f.o.} = 100 MeV$.

To make our investigations more realistic we have to take into account that only about 60% of J/Ψ measured are directly produced during collision. The rest is the result of χ ($\sim 30\%$) and ψ' ($\sim 10\%$) decay [20]. Therefore the realistic J/Ψ survival factor should read

$$\mathcal{N}(\epsilon_0) = 0.6\mathcal{N}_{J/\psi}(\epsilon_0) + 0.3\mathcal{N}_{\chi}(\epsilon_0) + 0.1\mathcal{N}_{\psi'}(\epsilon_0), \quad (21)$$

where $\mathcal{N}_{J/\psi}(\epsilon_0)$, $\mathcal{N}_\chi(\epsilon_0)$ and $\mathcal{N}_{\psi'}(\epsilon_0)$ are given also by formulae (4 -15) but with $\langle p_T^2 \rangle_{J/\Psi}^{AB}(\epsilon) = \langle p_T^2 \rangle_{J/\Psi}^{AB}(\epsilon)$, $\langle p_T^2 \rangle_\chi^{AB}(\epsilon)$, $\langle p_T^2 \rangle_{\psi'}^{AB}(\epsilon)$, $K_{J/\psi} = K_{J/\psi}$, K_χ , $K_{\psi'}$, $\sigma_{J/\psi N} = \sigma_{J/\psi N}$, $\sigma_{\chi N}$, $\sigma_{\psi' N}$ and $M = M_{J/\psi}$, M_χ , $M_{\psi'}$ respectively. The remaining problem is whether formula (5) is valid for χ and ψ' . There are data for $\langle p_T^2 \rangle_{\psi'}^{PbPb}$ [28] and they shows that $\langle p_T^2 \rangle_{\psi'}^{PbPb} \approx 1.4 \langle p_T^2 \rangle_{J/\Psi}^{PbPb}$. So, we assume that the above is also true for $\langle p_T^2 \rangle_{\psi'}^{AB}(\epsilon)$, i.e.

$$\langle p_T^2 \rangle_{\psi'}^{AB}(\epsilon) = 1.4 \langle p_T^2 \rangle_{J/\Psi}^{AB}(\epsilon) \quad (22)$$

with $\langle p_T^2 \rangle_{J/\Psi}^{AB}(\epsilon)$ given by (5) . For χ we believe that the inequality

$$\langle p_T^2 \rangle_{J/\Psi}^{AB} \leq \langle p_T^2 \rangle_\chi^{AB} \leq \langle p_T^2 \rangle_{\psi'}^{AB} \quad (23)$$

should be valid and therefore assume that (22) is true also in this case. Anyway, the exact form of $\langle p_T^2 \rangle_\chi^{AB}(\epsilon)$ or $\langle p_T^2 \rangle_{\psi'}^{AB}(\epsilon)$ is not very important because we checked that the suppression depends on this form very weakly. First, we put $K_{J/\psi} = 0$ and the resulting J/Ψ survival factor (for direct J/Ψ 's) differs only a few percent for the highest ϵ_0 from the one calculated with formula (5) unchanged. Second, when we use expression (5) also for χ and ψ' , the evaluated suppression factor is the same as that calculated with the use of (22), as far as plots are concerned.

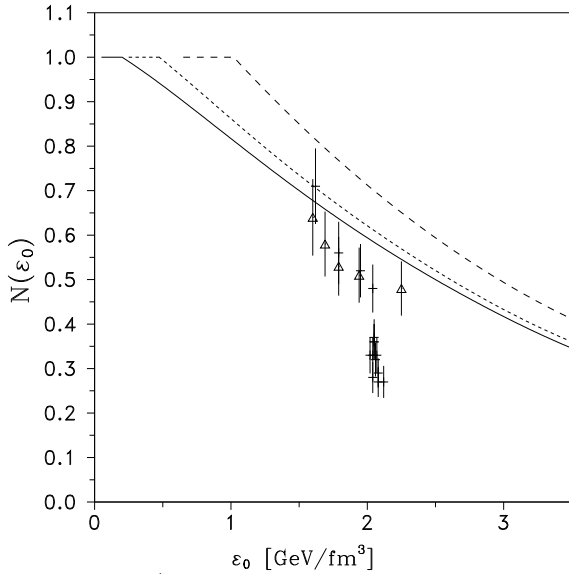


FIG. 6. J/Ψ suppression in the longitudinally expanding hadron gas with the "infinite" transverse size and for $\sigma_b = 4 \text{ mb}$, $\sigma_m = 2.66 \text{ mb}$ and $T_{f.o.} = 140 \text{ MeV}$. The curves correspond to $n_B^0 = 0.05 \text{ fm}^{-3}$ (solid), $n_B^0 = 0.25 \text{ fm}^{-3}$ (short-dashed) and $n_B^0 = 0.65 \text{ fm}^{-3}$ (dashed). Triangles and crosses represent the S-U data of NA38 and the Pb-Pb data of NA50 Collaborations [7], respectively.

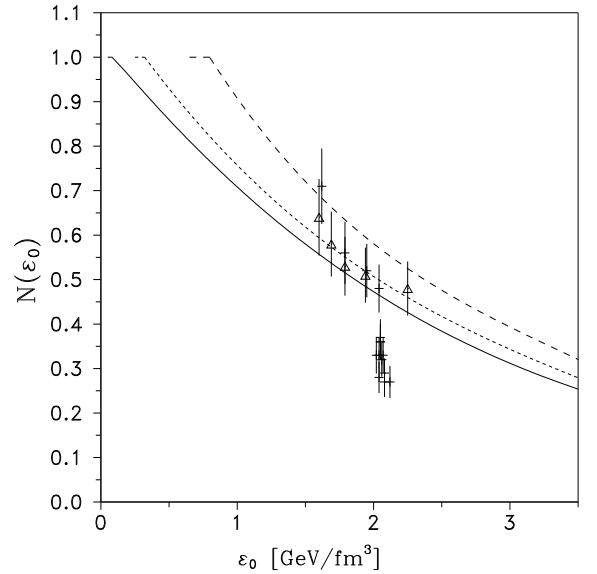


FIG. 7. Same as Fig. 6 but for $T_{f.o.} = 100 \text{ MeV}$.

To complete our estimations we need also values of cross-sections for $\chi - baryon$ and $\psi' - baryon$ scatterings (we will still hold that $\chi(\psi') - meson$ cross-section is $\frac{2}{3}$ of $\chi(\psi') - baryon$ cross-section). Since J/Ψ is smaller than χ or ψ' , $\chi - baryon$ and $\psi' - baryon$ cross-sections should be greater than $J/\Psi - baryon$ one. For simplicity, we assume that all these cross-sections are equal. This means that we *underestimate* J/Ψ suppression, here. The final results of calculations of (13) are presented in Figs. 4-7 for various sets of parameters of our model (which are $T_{f.o.}$, n_B^0 , σ_b). We performed these calculations for two values of $T_{f.o.} = 100, 140 \text{ MeV}$ which agree fairly well with values deduced from hadron yields [26]. For comparison, also the experimental data are shown in Figs. 4-7. The experimental survival factor is defined as

$$\mathcal{N}_{exp} = \frac{\frac{B_{\mu\mu} \sigma_{J/\psi}^{AB}}{\sigma_{DY}^{AB}}}{\frac{B_{\mu\mu} \sigma_{J/\psi}^{pp}}{\sigma_{DY}^{pp}}} , \quad (24)$$

where $\frac{B_{\mu\mu}\sigma_{J/\psi}^{AB(pp)}}{\sigma_{DY}^{AB(pp)}}$ is the ratio of the J/Ψ to the Drell-Yan production cross-section in A-B(p-p) interactions times the branching ratio of the J/Ψ into a muon pair. The values of the ratio for p-p, S-U and Pb-Pb are taken from [7]. Note that since the equality $\sigma_{DY}^{AB} = \sigma_{DY}^{pp} \cdot AB$ has been confirmed experimentally up to now [28], formula (24) reduces to

$$\mathcal{N}_{exp} = \frac{\sigma_{J/\psi}^{AB}}{AB\sigma_{DY}^{pp}}, \quad (25)$$

which is also given as the experimental survival factor, for instance, in [29].

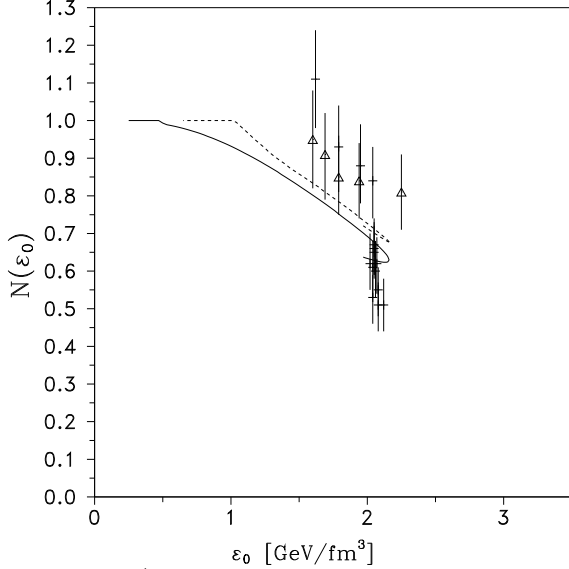


FIG. 8. J/Ψ suppression in the longitudinally and transversely expanding hadron gas for the uniform nuclear matter density distribution and $\sigma_b = 4 mb$, $\sigma_m = 2.66 mb$ and $T_{f.o.} = 140 MeV$. The curves correspond to $n_B^0 = 0.25 fm^{-3}$, $c_s = 0.45$ (solid) and $n_B^0 = 0.65 fm^{-3}$, $c_s = 0.46$ (dashed). Triangles and crosses represent the S-U data of NA38 and the Pb-Pb data of NA50 Collaborations [7] respectively, but the data are "cleaned out" from the contribution of J/Ψ scattering in the nuclear matter, in accordance with (26)

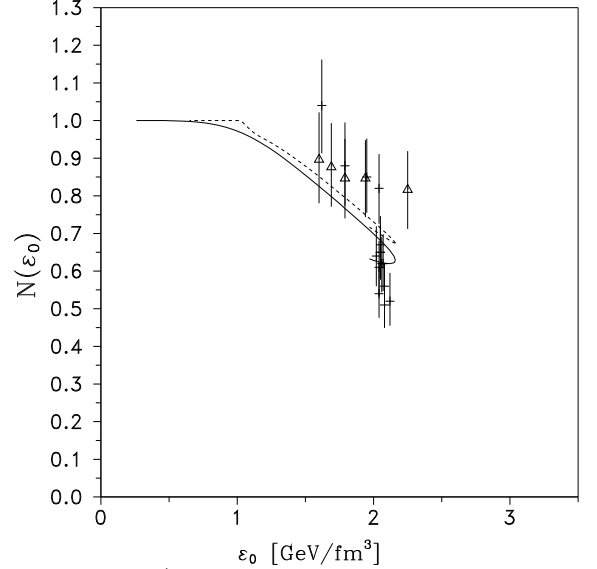


FIG. 9. J/Ψ suppression in the longitudinally and transversely expanding hadron gas for the Woods-Saxon nuclear matter density distribution and $\sigma_b = 4 mb$, $\sigma_m = 2.66 mb$ and $T_{f.o.} = 140 MeV$. The curves correspond to $n_B^0 = 0.25 fm^{-3}$, $c_s = 0.45$ (solid) and $n_B^0 = 0.65 fm^{-3}$, $c_s = 0.46$ (dashed). Triangles and crosses represent the S-U data of NA38 and the Pb-Pb data of NA50 Collaborations [7] respectively, but the data are "cleaned out" from the contribution of J/Ψ scattering in the nuclear matter, in accordance with (26)

Coming back to examination of our first results presented in Figs. 4-7, we can see that the most of Pb-Pb data are below the region of suppression obtained for chosen values of parameters in our model. Generally, the theoretical curves decrease slower with increasing ϵ_0 , whereas the data show rather abrupt fall just above $\epsilon_0 = 2 GeV/fm^3$. Note that the dependence on the initial baryon number density is substantial but for higher values of n_B^0 , rather. The lower the initial baryon number density, the deeper the suppression. There are two reasons for such a behaviour: the first, for the higher baryon number density, there are less non-strange heavier mesons ρ , ω in the hadron gas of the same ϵ_0 , but these particles create the most weighty fraction of scatters, for which reaction (1) have no threshold at all; the second, the freeze-out time $t_{f.o.}$ decreases with increasing n_B^0 for a given ϵ_0 in our model. For instance, for $\epsilon_0 = 3.5 GeV/fm^3$ and $T_{f.o.} = 140 MeV$ we have $a = 0.172, 0.175, 0.183$ and $t_{f.o.} = 15.7, 14.7, 11.6 fm$ for $n_B^0 = 0.05, 0.25, 0.65 fm^{-3}$, respectively. We can see also that the value $\sigma_b = 3mb$ is too small to obtain results comparable with the data, so we will leave aside this value in further investigations.

Now we will include the finite-size effects into our model, i.e. we will take into account that the realistic hadron gas has a finite transverse size. This will be done in form of the rarefaction wave moving inward S_{eff} with the sound velocity c_s . How to obtain this velocity has been mentioned in Sec.2 (see also [12]). With the finite-size effects included, the final expression for J/Ψ survival factor $\mathcal{N}_{h.g.}(\epsilon_0)$ will be given by (15). To make our investigations much more realistic we will also include the possible J/Ψ disintegration in nuclear matter, which should increase J/Ψ

suppression by about 10% [21]. But to draw also S-U data in figures, instead of multiplying $\mathcal{N}_{h.g.}$ by $\mathcal{N}_{n.m.}$ given by (7), we divide \mathcal{N}_{exp} by appropriate $\mathcal{N}_{n.m.}$, i.e. we define "the experimental J/Ψ hadron gas survival factor" as

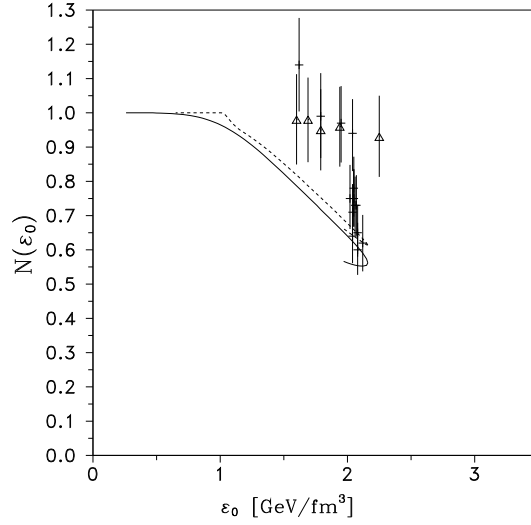


FIG. 10. Same as Fig. 9 but for $\sigma_b = 5 mb$, $\sigma_m = 3.33 mb$.

$$\tilde{\mathcal{N}}_{exp} = \exp \{ \sigma_{J/\psi N} \rho_0 L \} \cdot \mathcal{N}_{exp} . \quad (26)$$

and values of this factor are drawn in Figs. 8-10 as the experimental data. At the beginning we will consider a uniform nuclear matter density

$$\rho_A(\vec{s}, z) = \rho_A(\vec{r}) = \begin{cases} \rho_0 = \left(\frac{4\pi}{3} r_0^3\right)^{-1}, & |\vec{r}| \leq R_A \\ 0, & |\vec{r}| > R_A \end{cases} . \quad (27)$$

The results of numerical estimations of (15) and (26) are depicted in Fig. 8 for two values of the initial baryon number density, $n_B^0 = 0.25, 0.65 fm^{-3}$. The curve for $n_B^0 = 0.05 fm^{-3}$ almost covers the curve for $n_B^0 = 0.25 fm^{-3}$ and the maximal difference between these curves do not exceed 1.9% (which is the difference for the highest possible ϵ_0 , i.e. $\epsilon_0 \approx 2 GeV/fm^{-3}$), so for clearness of the figure we do not draw it. The two values of the speed of sound are the maximal values of this quantity possible in the range $[T_{f.o.} = 140 MeV, T_{0,max}]$ for the above-mentioned two cases of n_B^0 . In fact, we have checked that the results almost do not depend on c_s (allowed in the range) and the difference (seen only for the quantity ϵ_0) between J/Ψ survival factors for the maximal and the minimal values of c_s in the range $[T_{f.o.} = 140 MeV, T_{0,max}]$ are less than 0.6%. Note that the theoretical curves in Figs. 8 (the same will happen in Figs. 9-10) are two-valued around $\epsilon_0 = 2 GeV/fm^{-3}$. This is the result of our approximation of $\epsilon_0(b)$ given by (19). This expression allows for two different values of b , which give the same ϵ_0 in some range of the impact parameter (see Sec.4).

It has turned out also that in the case of the transverse expansion, the results almost do not depend on the $T_{f.o.}$ (for $T_{f.o.} \in [100, 140] MeV$). And the maximal difference (seen for the quantity ϵ_0) between curves for $T_{f.o.} = 100 MeV$ and $T_{f.o.} = 140 MeV$ do not exceed 2.7% ($n_B^0 = 0.05 fm^{-3}$), 2.6% ($n_B^0 = 0.25 fm^{-3}$). This is because the freeze-out time resulting from the transverse expansion, $t_{f.o.,trans} = R_A/c_s$ (if we assume a central collision and c_s constant), is of the order of the freeze-out time resulting from the longitudinal expansion for $T_{f.o.} = 140 MeV$. Namely, for Pb and $c_s = 0.45$ we have $t_{f.o.,trans} \cong 15.8 fm$ which is very similar to values of $t_{f.o.}$ for $T_{f.o.} = 140 MeV$ given earlier. For $T_{f.o.} = 100 MeV$, $t_{f.o.} = 111.0, 101.0, 72.5 fm$ for $n_B^0 = 0.05, 0.25, 0.65 fm^{-3}$ respectively, so the hadron gas ceases because of the transverse expansion much earlier.

We repeated our estimations of formula (15) also for the more realistic nuclear matter density distribution, namely for the Woods-Saxon distribution with parameters taken from [30]. The results are presented in Figs. 9-10. We can see that these curves fit the data a little bit better than those obtained within the assumption of the uniform nuclear matter density distribution (cf. Fig. 8 and 9). Generally, taking into account also the transverse expansion changes the final (theoretical) pattern of J/Ψ suppression qualitatively. First of all, the curves for the case including the transverse expansion are concave (what is more clearly seen for lower n_B^0) as the data suggest should be, in opposite to the case with the longitudinal expansion only, where curves are convex. But still, theoretical curves are not steep enough to cover the data area completely. We would like to note at this point that there is some ambiguity in

calculation of $\langle E_T \rangle$ and b in NA50 experiment, since the range of ϵ_0 obtained from (16) with the use of $\langle E_T \rangle$ and b for 1995 and 1996 Pb-Pb runs are different. For 1995 run [31] we have $\epsilon_0 \cong 2.6 - 2.9 \text{ GeV}/fm^{-3}$ and for 1996 run [7] $\epsilon_0 \cong 2.0 - 2.1 \text{ GeV}/fm^{-3}$, both estimates are for $\langle E_T \rangle \geq 40 \text{ GeV}$. Of course, where exactly the data points should be placed is crucial for the valuation of the correctness of the shape of theoretical curves.

When the additional disintegration in the nuclear matter is included, also the magnitude of J/Ψ suppression is comparable with the data, but rather for greater σ_b . But note that since we have one overall charmonium-baryon cross-section σ_b , our final results underestimate the suppression (for χ^- , ψ' - baryon scattering the cross-section should be greater than for J/Ψ).

As a final remark, we think that it is difficult to exclude J/Ψ scattering in the hot hadron gas entirely, as the reason for the observed J/Ψ suppression at this point. In our model the most crucial parameter is the charmonium-baryon inelastic cross-section and the final results depend on its value substantially. Therefore it is of the greatest importance to establish how this cross-section behaves in the hot hadron environment. Some work has been done into this direction [32–34], but results presented there differ from each other and are based on different models.

ACKNOWLEDGEMENTS

We would like to thank Dr K.Redlich for very helpful discussions.

-
- [1] T.Matsui and H.Satz, Phys.Lett.B **178**,416 (1986)
 - [2] J.Ftáčnik, P.Lichard and J.Pišút, Phys.Lett.B **207**, 194 (1988)
 - [3] R.Vogt, M.Prakash, P.Koch and T.H.Hansson, Phys.Lett.B **207**, 263 (1988)
 - [4] S.Gavin, M.Gyulassy and A.Jackson, Phys.Lett.B **207**, 257 (1988)
 - [5] J.-P. Blaizot, J. Ollitrault, Phys. Rev. D **39**, 232 (1989)
 - [6] D. Prorok, L. Turko, Z.Phys. C **61**, 109 (1994)
 - [7] M.C. Abreu et al. (NA38), Phys. Lett. B **449**, 128 (1999); M.C. Abreu et al. (NA50), Phys. Lett. B **450**, 456 (1999)
 - [8] J.D. Bjorken, Phys. Rev. D **27**, 140 (1983)
 - [9] J. Cleymans, R.V. Gavai, E. Suhonen, Phys. Rep. **130**, 217 (1986)
 - [10] G. Baym, B.L. Friman, J.-P. Blaizot, M. Soyeur, W. Czyż, Nucl. Phys. A **407**, 541 (1983)
 - [11] D. Prorok, L. Turko, Z.Phys. C **68**, 315 (1995)
 - [12] D. Prorok, L. Turko, in preparation
 - [13] J. Hüfner, Y. Kurihara, H.J. Pirner, Phys. Lett.B **215**, 218 (1988)
 - [14] S. Gavin, M. Gyulassy, Phys. Lett. B **214**, 241 (1988)
 - [15] J.-P. Blaizot, J.-Y. Ollitrault, Phys. Lett. B **217**, 392 (1989)
 - [16] J. Badier et al. (NA3), Z. Phys. C **20**, 101 (1983)
 - [17] S. Gupta, H. Satz, Phys. Lett. B **283**, 439 (1992)
 - [18] C. Baglin et al. (NA38), Phys. Lett. B **268**, 453 (1991)
 - [19] D. Kharzeev, C. Lourenço, M. Nardi, H. Satz, Z. Phys. C **74**, 307 (1997)
 - [20] H. Satz, hep-ph/9711289, Nov. 1997
 - [21] C. Gerschel, J. Hüfner, Phys. Lett. B **207**, 253 (1988)
 - [22] S. Gavin, R. Vogt, Phys. Rev. Lett. **78**, 1006 (1997)
 - [23] C. Gerschel, J. Hüfner, Z. Phys. C **56**, 171 (1992)
 - [24] S. Gavin, hep-ph/9609470, Sep. 1996
 - [25] H. Ströbele (NA35), Nucl. Phys. A **525**, 59c (1991)
 - [26] J. Stachel, Nucl. Phys. A **654**, 119 (1999)
 - [27] L. Ahle et al. (E-802), Phys. Rev. C **57**, R466 (1998)
 - [28] M. C. Abreu et al. (NA50), Nucl. Phys. A **638**, 261c (1998)
 - [29] C. Lourenço, Nucl. Phys. A **610**, 552c (1996)
 - [30] C. W. de Jager, H. de Vries, C. de Vries, Atomic Data and Nuclear Data Tables **14**, 479 (1974)
 - [31] M. C. Abreu et al. (NA50), Phys. Lett. B **410**, 327 (1997)
 - [32] D. Kharzeev, H. Satz, Phys. Lett. B **334**, 155 (1994)
 - [33] K. Martins, D. Blaschke, E. Quack, Phys. Rev. C **51**, 2723 (1995)
 - [34] S. G. Matinyan, B. Müller, Phys. Rev. C **58**, 2994 (1998)